SAGE
Publishing

Research Article

Removal of Azo Dye Carmoisine by Adsorption Process on Diatomite

Kotbia Labiod [1,2] Sabir Hazourli,[1] Marwa Bendaia,[1] Mohamed Tlili,[3] Adel AitBara,[4] Radouane Graine,[2] and Hazem Meradi[2]

[1]*Laboratory of Water Treatment and Valorization of Industrial Wastes, Chemistry Department, Faculty of Sciences, Badji-Mokhtar University, Bp12, 23000 Annaba, Algeria*
[2]*Research Center in Industrial Technologies, CRTI, P.O. Box 64, Cheraga, 16014 Algiers, Algeria*
[3]*Laboratory of Desalination and Natural Water Valorization-CERTE, Borj-CédriaTechnopole BP 273-8020 Soliman, Tunisia*
[4]*Laboratory of Physical Chemistry of Materials, Department of Chemistry, Faculty of Sciences and Technology, Chadli Bendjedid University, B.P. 36, El Tarf 36000, Algeria*

Correspondence should be addressed to Kotbia Labiod; labiodkotbia@yahoo.fr

Received 29 March 2022; Revised 2 August 2022; Accepted 12 August 2022; Published 9 September 2022

Academic Editor: Sami-Ullah Rather

This work aims to evaluate the adsorption capacity of an abundant natural diatomite (ND) to remove the azo dye carmoisine, known as a harmful emerging organic pollutant. Indeed, to the best of our knowledge, no results were reported on this subject. The ND was characterized by FTIR, XRD, and SEM/EDX analyses. The experimental study of adsorption was carried out in batch mode. Results showed that ND adsorbent is mainly composed of silica. A fraction of calcite and ankerite was also identified. It is a porous material with a specific surface of about $41 \text{ m}^2 \cdot \text{g}^{-1}$ and with a hydroxyl surface functional group -OH. Adsorption results showed that adsorption process on ND is found to be effective in removing the carmoisine colorant. The adsorption capacity is strongly affected by the adsorbent and adsorbate contents, the solution pH, the work temperature, and the water hardness and mineralization. At room temperature, optimal experimental conditions for the highest adsorption capacity ($12 \text{ mg} \cdot \text{g}^{-1}$) were colorant concentration $50 \text{ mg} \cdot \text{L}^{-1}$, pH 2, contact time 30min, and ND content $1 \text{ g} \cdot \text{L}^{-1}$. Modeling study has showed that experimental results are well modeled by the Freundlich isotherm in multilayer adsorption. The reaction kinetics are pseudo-second order, and the thermodynamic parameters indicated that the nature of the adsorption process is endothermic and spontaneous.

1. Introduction

Azoic dyes make up most dyes used in food, textiles, plastics, etc. Their productions and commercialization continue to increase, and they constitute 50-70% of the synthetic dyes used for industrial purposes [1, 2]. However, the release of these recalcitrant dyes, done generally in the water bodies directly, characterizes an important way of environmental contamination [3]. They are harmful to humans, aquatic fauna, and flora [4, 5]. Several methods and techniques were then proposed to treat contaminated water and wastewater. It was reported that the biological treatments under aerobic conditions are not often effective due to the recalcitrance to the degradation of some dyes [6]. Nevertheless, physico-chemical processes such as coagulation-flocculation, electro-coagulation, membrane techniques, and chemical and electrochemical oxidation have shown excellent efficacy in treating azo dyes [7–9]. The adsorption, as process of pollutant removal, is chosen for this study; it can be also an alternative method for the treatment of contaminated water with organic molecule as azo dyes. The adsorption process consists in removing the pollutant from the aqueous phase and concentrating it in the adsorbent surface following several mechanisms. It is known to be an efficient, relatively simple, and inexpensive technique. Different adsorbents can be used: classic such as activated carbon and silica gel, as well as recent ones such as natural and industrial waste [10–12]. Natural diatomite (ND) can be also considered

among these recent adsorbents, which meet the criteria of sustainable development. ND is an accumulation of hydrated amorphous silica of high stability, nontoxic, low density, and naturally porous [13]. Several researches were performed for possible applications in various domain such as catalysis, hydrogen storage, thermal energy storage, and solar energy production [14–16]. Moreover, ND is recognized to have an adsorbent power for many pollutants [17]. In water treatment and more particularly for the adsorption of dyes, diatomite has also been applied [18–21]; but the literature review has not shown any report on carmoisine dye. In the present work, the study of carmoisine removal was motivated by the fact that it is a very common azo dye, incorporated into several food products: juices, sodas, cookies, ice cream, canned fruits, red meats, etc. [22, 23], making it a potential pollutant which can be released in the environment. In addition, carmoisine, like all other azo dyes, is stable and difficult to degrade; then it can cause more or less serious health risks, such as hyperactivity and attention disorders in children and also neurological and allergenic potentials [24]. For the specific treatment of food dyes, different techniques were applied for wastewater and synthetic solutions: a rotating activated carbon adsorber [25], hybrid system coupling electrocoagulation and solar photocatalysis [26], microbial degradation [27], electro-oxidation-plasma [28], Fenton process [29], and electrocoagulation [30]. Hence, this study will focus on the removal of carmoisine azo dye by adsorption process on natural diatomite. Indeed, there is no work in the literature on this adsorbent/adsorbate couple. For this, the study will start by a physicochemical characterization of the ND adsorbent. In a second stage, main parameters that control adsorption treatment process will be optimized in a batch mode. Finally, modeling of adsorption isotherm and adsorption kinetics will be performed.

2. Materials and Methods

2.1. Preparation and Characterization of Diatomite for Adsorption. The adsorbent used in this study is ND from the Sig region (west Algeria). The raw diatomite without prior pretreatment was washed several times with bidistilled water until the turbidity of the rinse water was less than 5 NTU. After removing the impurities, the diatomite was dried in a study at 80°C for 24 h and then weighed several times until constant weight to evaporate moisture. The dry diatomite was milled (grinder Janke and Kunkel IKA Labortechnik) to obtain a grain size around 1 mm. The resulting sample was kept in an airtight bottle for later use in characterization and the adsorption tests. The characterization of a material is an important factor in explaining the adsorption mechanism. Thus, different structure and texture parameters of an ND were examined. It is possible to cite the specific surface analyzed by nitrogen adsorption at 77°K, using an instrument Thermo Quest Sorptomatic1990, according to the traditional method of Brunauer, Emmett, and Teller or BET [31]. The Fourier transform infrared (FTIR) spectroscopy was recorded at room temperature between 400 and 4000 cm^{-1} by the standard KBr disk method using a Shi-

madzu spectrometer. The scanning electron microscopy (SEM) was employed to visualize the morphology of ND using a Philips XL-3 CP microscope. The X-ray diffraction (XRD) was performed on an X-ray diffractometer (Philips X'PERT PANalytical, Almelo, Pays-Bas) with a radiation CuKα at $\lambda = 1.54$ Å, operating at 50.0 kV and 200.0 mA. The point of zero charge (PZC) was carried out from 50 mL of 0.1 M NaCl solutions transferred in a series of beakers 100 mL. A mass of 0.1 g of ND was added to each beaker for stirring of the suspension for 24 h. The final pH is measured to determine the PZC of ND by plotting the pH final-pH initial curve vs. initial pH [10].

2.2. Preparation and Analysis. For the preparation and the analyses, we followed the approach of [32, 33].
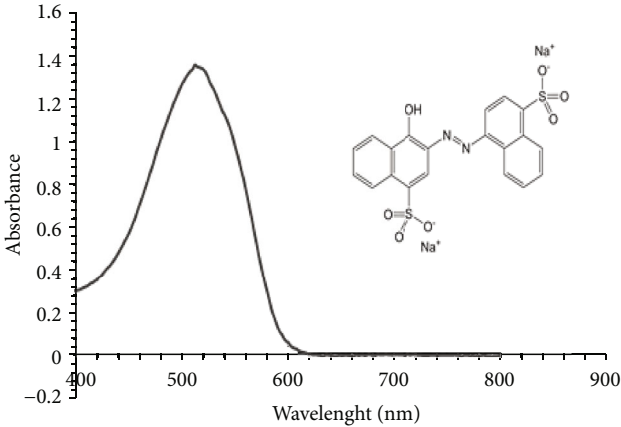
2.2.1. Preparation. The food colorant tested in this study is a commercial dye prepared in synthetic aqueous solution, and some specific characteristics of this dye are given in (Table 1). All the reagents used for pH regulation in solution (NaOH and HCl) and others are analytical grade supplied by Panreac and Sigma. These reagents are prepared at the desired concentration in double-distilled water.

For the purposes of calibration and adsorption tests, a stock solution of carmoisine at 50 mg L^{-1} was prepared by dissolving its powder in double-distilled water. Scanning this solution in the visible spectrum between 400 and 800 nm made it possible to determine the maximum wavelength (λmax: 512 nm). The calibration was carried out at this wavelength for the daughter concentrations: 5, 10, 20, 30, and 40 mg L^{-1} prepared by dilution of the stock solution to 50 mg L^{-1}. It should be noted that the correlation coefficient of the calibration curve obtained from the concentration measurements of these solutions is close to unity.

2.2.2. Analysis. The absorbance measurements of all the carmoisine solutions prepared before and after adsorption were carried out using a single-beam type UV/visible spectrophotometer (Spectrophotometer Jenway 7315).

2.3. Batch Adsorption Experiments. The adsorption tests of carmoisine on ND were conducted in batch mode. In order to find the best operating conditions, the influence of important parameters in the adsorption phenomena, was tested. The parameters are as follows: the initial concentration of ND (0.25 to 5 g L^{-1}), the initial pH of the solution (2 to 9), the initial concentration of carmoisine (5 to 60 mg L^{-1}), and the initial temperature of the solution (10 to 50°C). For pH tests, the solutions were adjusted using 0.1 M HCl or NaOH. For all experiments, a considered mass of ND is contacted with 50 mL of the carmoisine solution in a 100-mL beaker. This mixture was stirred in a thermoregulated bath at a constant speed of 200 rpm for a definite contact time. After the adsorption equilibrium, the contents of the beaker are filtered, and the residual concentration of carmoisine is measured in visible spectrometry at 512 nm. The absorption capacity of carmoisine on ND at equilibrium (qe: mg L^{-1})

TABLE 1: Some characteristics of carmoisine used.

Molecular formula: $C_{10}H_{12}N_2Na_2O_7S_2$	Molecular structure and visible spectrum for concentration 50 mg L^{-1} at free pH
Synonyms: Azorubine, Acid Red 14	
C.I. number: C.I. 14720	
Code E: E122	
Red color powder (KUHIMANN 99%)	
Food dye, monoazo, anionic	
Weight: 502.44 g moL^{-1}	
Water solubility: 120 g L^{-1}	
λmax: 512 nm	
Free pH: 7.56	

can be formulated by

$$qe = \frac{(Co - Cf)}{m} . V,$$ (1)

where C_o and C_f are the initial and equilibrium concentration measurement values of carmoisine in solution, V (L) is the volume of the carmoisine in solution to be treated, and m (g) is the weight of ND.

For each measurement realized (5 series), the relative error is less than 5%. In order to validate the experimental results, kinetic models pseudo-first order [34] and pseudo-second order [35], as well as the adsorption isotherms [36, 37], were applied. To find the adsorption isotherms and kinetic models best adapted, it is necessary to analyze all the data using chi-square (χ^2) but also correlation coefficients (R^2). The chi-square can be represented by

$$\chi2 = \sum \frac{(qee - qec)2}{qec},$$ (2)

where q_{ee} is the experimental data of equilibrium capacity (mg g^{-1}) and q_{ec} is equilibrium capacity obtained by calculating from a model (mg g^{-1}).

For a low value of χ^2, it can be deduced that the experimental data are adapted to the proposed model.

2.4. Study of Material Regeneration and Wear. The adsorption/desorption or regeneration experiments were performed by saturating 10 g of ND with carmoisine. This is achieved by inserting into different beakers, 1 g L^{-1} of ND with 50 mL of carmoisine at 50 mg L^{-1} and pH 2. After stirring the mixture for an equilibrium time of 60 min at 200 rpm, the ND masses are recovered by filtration to be dried in an oven (Memmert) at 105°C for 5 hours. For the desorption tests, masses of ND saturated with carmine are transferred into different eluents: bidistilled water and solutions at a concentration of 0.1 M: HCl, H_2SO_4, H_3PO_4, CH_3COOH, and NaOH. Organic solvents were also used: ethanol and acetone at 25, 50, and 75% successively. These

desorption tests were carried out at a stirring speed of 200 rpm and at a temperature of 20°C, for a contact time of 60 min. Material wear was deduced from repeated adsorption/desorption tests or regeneration cycles using the best eluent.

3. Results and Discussion

3.1. Characterization of ND Material. In order to achieve optimal performance in terms of adsorption capacity, it is essential to have a suitable adsorbent material that meets the criteria of cost and adsorbability [38, 39].

Thus, the characterization of a material is necessary before any study on surface treatments such as adsorption. Knowledge of the structure, texture, and chemical composition parameters would facilitate the understanding of the adsorption phenomena. For this purpose, several parameters were analyzed on the ND studied.

X-ray diffraction analysis indicates that ND contains minerals of calcite, quartz, and ankerite, as shown in Figure 1, These three phases are in the range of 30 to 85°of 2-theta. Their presence in a diatomite gives it to be used as a potential adsorbent [40].

The ND studied has a specific surface area (BET) of 40.1 m^{2}g^{-1}. This surface value is close to that found by [41] for a diatomite of the same locality, but a sampling place is probably different. It should be noted that according to regions and countries, variable specific surfaces are observed: low 13.04 m^{2}g^{-1} [42] and high 149 m^{2}g^{-1} [43].

Given the low specific surface areas found compared to those of activated carbons which can reach 2000 m^{2}g^{-1} [44], it can be deduced that the adsorption of dyes would be governed by the pores heterogeneity surface of the diatomite and/or the electrostatic effect via the surface sites of the material. These deductions have been observed for natural diatomites of different types and compositions [18, 20].

The microscopic structure of ND samples observed using SEM images shows a set of regular pores, aligned, and of different sizes according to a pattern of honeycomb in Figure 2. This figure reveals overlays layers of ND with
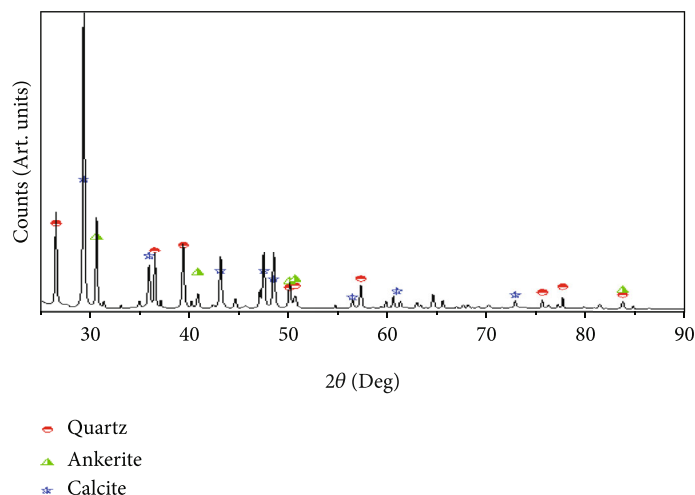
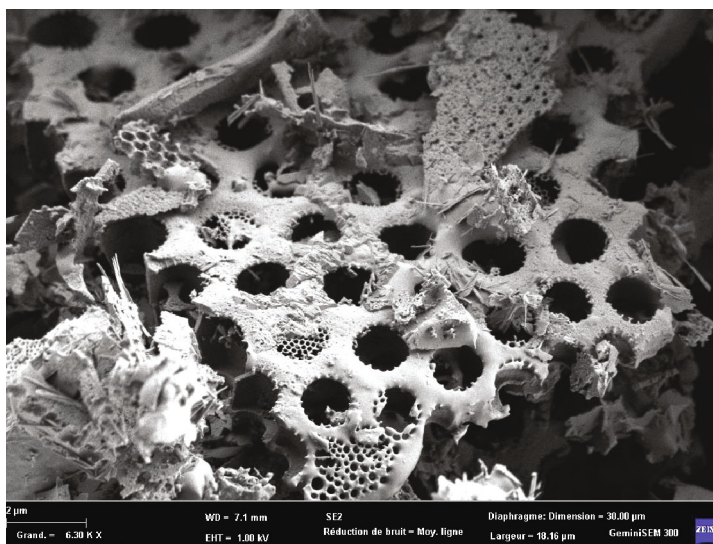FIGURE 1: X-ray diffraction patterns of ND.

FIGURE 2: SEM images of ND displaying surface morphology details.

clogging of a certain number of pores, in addition to impurities related to the natural origin of ND. According to [45], the presence of porosity in the diatomite gives it a high permeability and a high adsorption capacity. Figure 3 presents the weight composition of ND obtained by EDX. It reveals the presence of oxides of Si (31.28% in Si) and Al (1.78% in Al) and other mineral impurities, such as Na, Ca, Mg, and F.

In order to determine the surface groupings of ND that may be involved in the adsorption of the carmoisine, the IR spectrum was established. Figure 4 describes the main absorption bands found at 3419.79, 1797.66, 1431.18, 1095.57, 873.75, 798.53, 711.73, and 466.77 cm^{-1}. The wide band at 3419.79 cm^{-1} is due to the OH elongation vibration but could also be attributed to the Si-OH and Al-OH elongation vibrations groups as observed by [46] on a natural diatomite. The carbon bands at 1797.66 and 1431.18 cm^{-1} would

be the groups (C=O) and (CH$_3$) successively. The signal at 1095.57 cm^{-1} corresponds to the siloxane group (Si-O-Si), while the peak at 873.75 cm^{-1} would be related to the bending vibration of the Al-O-Si group (octahedral sheet) [47]. The 798.53 cm^{-1} band is attributed to the free silica and/or quartz found in all diatomites (Si-O-Si intertetrahedral bending). The peak at 711.73 cm^{-1} corresponds to the C-O bond of calcium carbonate belonging to diatomite. The band at 466.77 cm^{-1} can be defined as an asymmetric elongation mode of the Si-O-Si bond.

3.2. Operating Parameters

3.2.1. Effect of Adsorbent Concentration on Carmoisine Adsorption. Studying the effect of adsorbent concentration is important; this allows the optimum adsorption to be determined. In other words, identify the necessary and

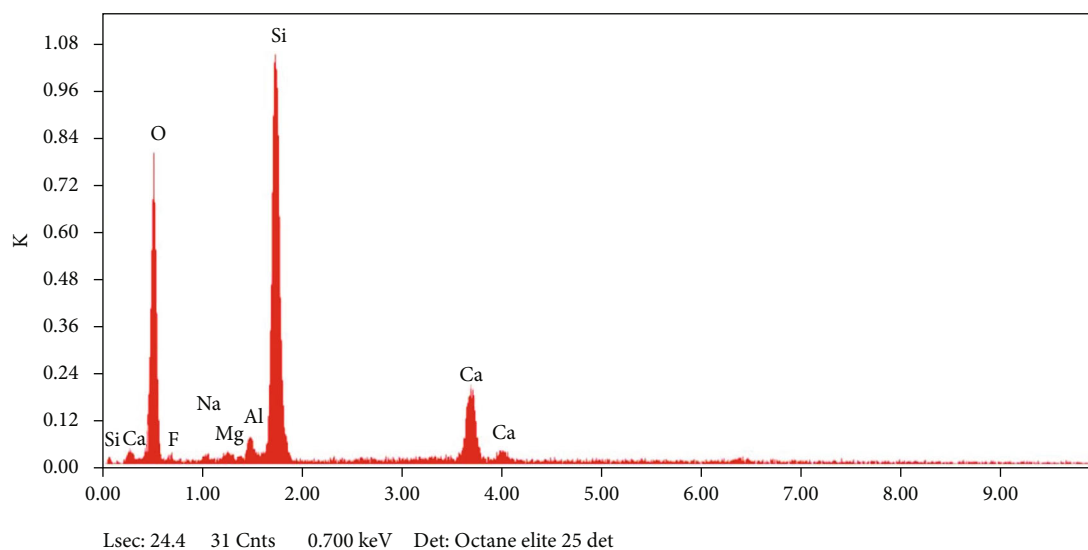Lsec: 24.4   31 Cnts   0.700 keV   Det: Octane elite 25 det
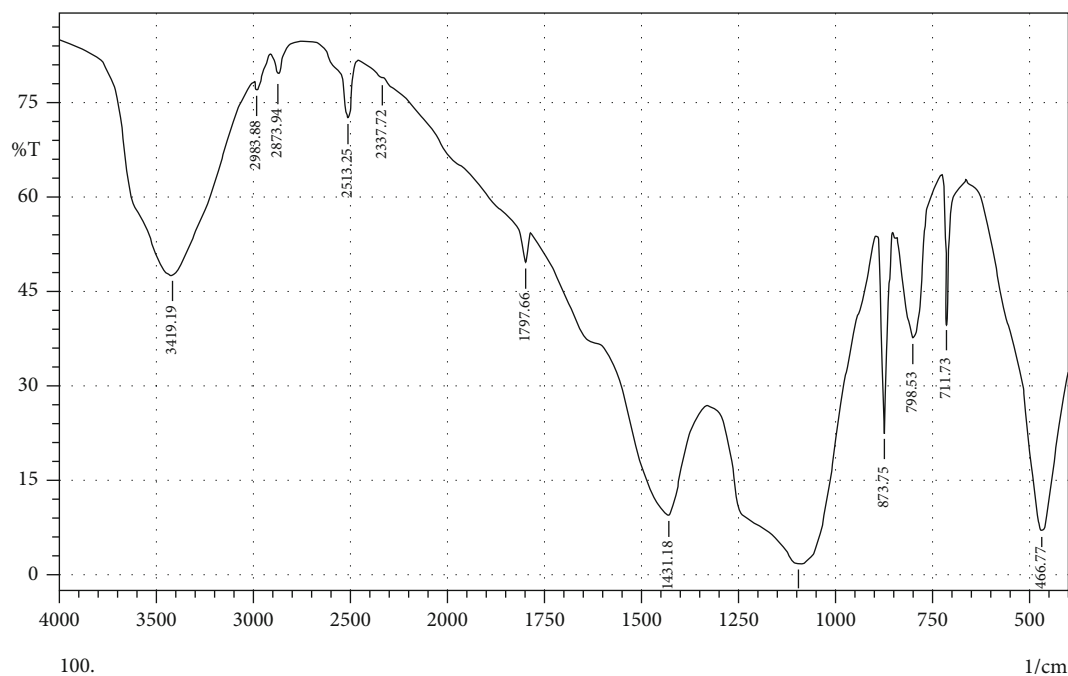
FIGURE 3: Composition of ND by EDX.

FIGURE 4: IR spectrum of ND.

sufficient quantity of adsorbent to obtain maximum adsorption capacity. Therefore, the higher the concentration of adsorbent used, the higher the cost of operation and vice versa [48].

In this study, the effect of ND concentration for the removal of carmoisine from an aqueous solution at $50 \, mgL^{-1}$, room temperature $21 \pm 0.5°C$, and $pH \, 2 \pm 0.1$ is illustrated in Figure 5. It can be observed that carmoisine reduction increases with increasing ND concentration. For the choice of the optimum concentration of ND to keep for the following experiments, $1 \, g \, L^{-1}$ is taken. This confers a maximum efficiency to the saturation in the carmoisine

material but also economically viable. The increase in carmoisine elimination over time and with the increase of ND concentration is attributed to the availability of more surfaces therefore more active sites for adsorption. For a residual *biomass* of Saccharomyces cerevisiae with carmoisine [4] and tea waste with Congo red [49], similar findings were reported.

3.2.2. Effect of Solution pH on Carmoisine Adsorption and Mechanisms. The pH parameter plays an important role on the surface charge of the adsorbent, on the degree of ionization of the dye in solution and consequently on the
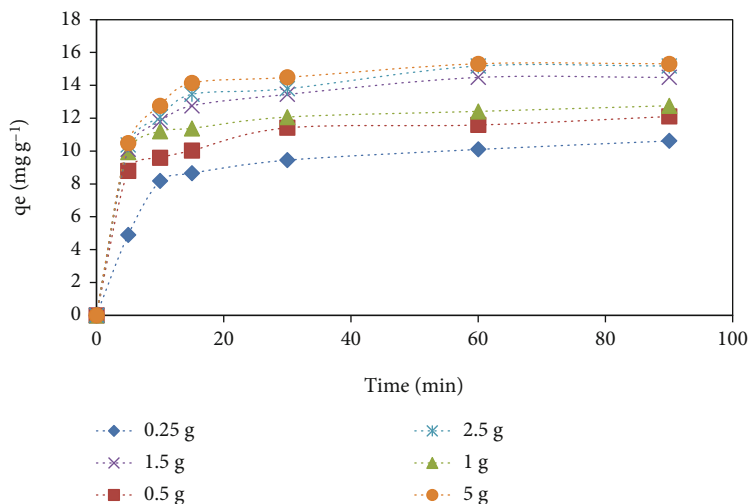
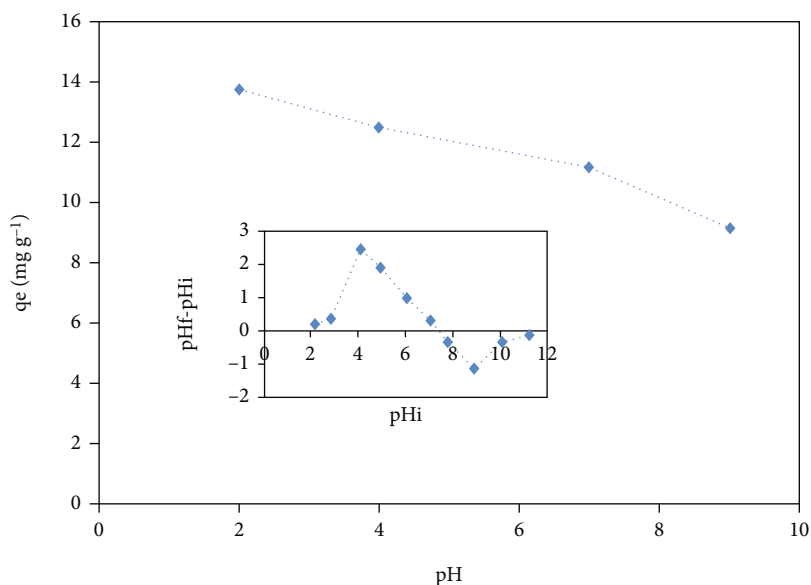FIGURE 5: Effect of ND concentration on adsorption of carmoisine.

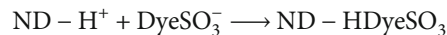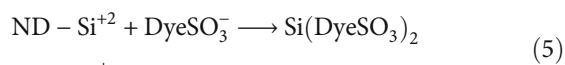FIGURE 6: Effect of the initial pH of the carmoisine solution on adsorption efficiency.

adsorption rate [50, 51]. The pH effect was studied at values between 2 and 9.

The other experimental parameters are kept constant at $1 \, g \, L^{-1}$ in ND, $50 \, mg \, L^{-1}$ of carmoisine, contact time at 60 min, and a temperature at $21 \pm 0.5°C$. The results given in Figure 6 show a decrease in the adsorption capacity of 14 to $9 \, mg \, g^{-1}$ for a pH ranging from 2 to 9. At low pH (lower than point of zero charge (PZC = 7.16), the ND surface is positively charged with aluminum and silica oxides in addition to protonation by H^+ ions from HCl. If it refers to the composition of most diatomites, it finds that the percentage of the siloxane group or SiO_2 prevails [47, 52]. Thus, the mechanism of adsorption of carmoisine can be considered by the electrostatic interactions between the SiO_2 groups of the surface of the ND and the sulfonates of carmoisine. In aqueous solution, SiO_2 can be decomposed into

Si^{+2} and O_2^{2-} on the surface of ND (Equation (3)), and carmoisine is dissociated into negatively charged sulfonates.

$$SiO_2 \longrightarrow Si^{+2} + O_2^{-2} \qquad (3)$$

$$DyeSO_3Na \longrightarrow DyeSO_3^- + Na^+ \qquad (4)$$
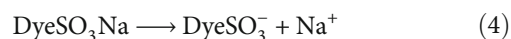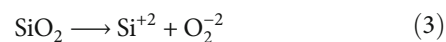
Thus, the important adsorption in acid medium could be formulated by the interactions of Si^{+2} and H^+ of the surface of the ND with the sulfonates in solution.

$$ND - Si^{+2} + DyeSO_3^- \longrightarrow Si(DyeSO_3)_2$$
$$ND - H^+ + DyeSO_3^- \longrightarrow ND - HDyeSO_3 \qquad (5)$$

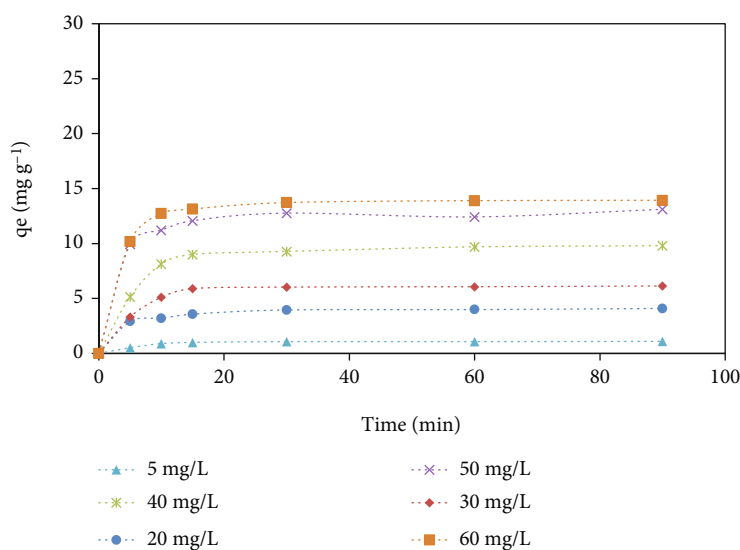On the other hand, at pH above the value of PZC, the

FIGURE 7: Effects of initial carmoisine concentration and contact time on adsorption efficiency.
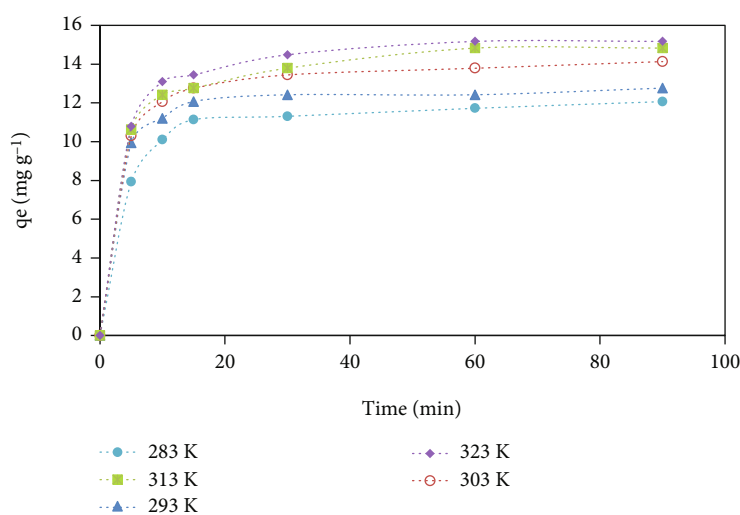

FIGURE 8: Effect of the initial temperature of the solution on the adsorption efficiency of carmoisine on ND.

surface of the ND becomes negatively charged, due to the predominance of OH⁻ resulting from the addition of NaOH. In addition, the presence of OH⁻ in solution may compete with the sulfonate groups thereby reducing the number of positive charges on the ND surface as the pH increases. In this case, electrostatic repulsion adsorbent/adsorbate is favored; diffusion and adsorption are then delayed. Similar results have been reported on the adsorption of carmoisine with "bottom ash and deoiled soya" [3] and "waste biomass of Saccharomyces cerevisiae" [4].

3.2.3. Effect of Contact Time and Initial Carmoisine Concentration on Adsorption. The effects of the contact time and the initial concentration of a given pollutant are very important for assessing the kinetics of the reaction [10].

This study was carried out at deferent concentrations of carmoisine and contact times between 5 to 60 mg L⁻¹ and 5

to 90 min, respectively. The concentration parameters of the adsorbent, the pH of the carmoisine solution, and the ambient temperature are kept constant at $1 \, g \, L^{-1}$, pH 2 ± 0.1, and $21 \pm 0.5°C$. The results presented in Figure 7 show that the adsorption capacity of carmoisine on ND increases with increasing dye concentration and contact time. It is also observed that the adsorption of carmoisine is rapid during the first 5 min and then tends to proceed slowly until about 30 min where the adsorption capacity is optimal for each of the concentrations tested. This adsorption capacity is approximately $12 \, mg \, g^{-1}$ for carmoisine initial concentrations of 50 and $60 \, mg \, L^{-1}$. Therefore, for all experiments, the dye concentration was chosen at $50 \, mg \, L^{-1}$, while the equilibrium time is set at 60 min to be reassured of the complete saturation of the ND. The increase in adsorption with the progression of carmoisine concentration is attributed to the decrease in adsorption resistance and the increase in
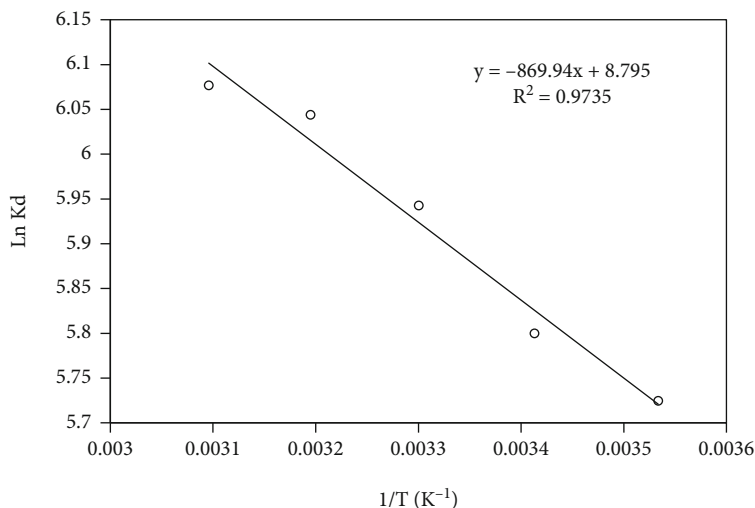
FIGURE 9: Van't Hoff plot for carmoisine adsorption on ND.

TABLE 2: Thermodynamic parameter values for carmoisine adsorption equilibrium on ND.

T (°C)	Thermodynamic equilibrium constant (Kd)	$\Delta G°$ (KJmol^{-1})	$\Delta S°$ (Jmol^{-1})	$\Delta H°$ (KJmol^{-1})
10	306.306	-13.46		
20	330.275	-14.19	73.12	7.23
30	380.952	-14.92		
40	421.568	-15.69		
50	435.643	-16.38		

TABLE 3: Some characteristics of the waters tested.

Nature of water	pH	Hardness (mg L^{-1}CaCO$_3$)	Conductivity (μs cm^{-1})
Bidistilled water	6.5	0	2.1
Sweet water	7.4	124	203
Drinking water	7.24	180	514
Very hard water	6.9	870	1800

the driving force of the concentration gradient for adsorbent/adsorbate mass transfer, more particularly the active sites of the adsorbent and the sulfonate groups of the dye. However, this driving force decreases with the adsorption time due to the progressive saturation of the adsorbent [53]. Similar results and behaviors have been reported by different authors [4, 8, 54].

3.2.4. Effect of the Initial Temperature of the Solution and Thermodynamic Study. The effect of temperature is another important physicochemical parameter in explaining the adsorption phenomenon because it modifies the mobility of the pollutant in solution and its adsorption capacity on the adsorbent as well as the thermodynamic process [55–57].
The adsorption of the carmoisine on ND was studied at different temperatures between 283 and 323°K and at con-

tact times between 0 and 90 min. The parameters of concentration of the adsorbent, the pH, and the initial concentration of the carmoisine solution are kept constant at $1 \, g \, L^{-1}$, pH 2 ± 0.1 and $50 \, mg \, L^{-1}$. The results presented in Figure 8 show that at the temperatures considered, the absorption capacity of carmoisine varies approximately between 13 and $16 \, mg \, g^{-1}$. This indicates that the adsorption of carmoisine on ND is endothermic nature. The increased adsorption with temperature can be attributed to the increased mobility of the dye molecules and the number of active surface sites available for adsorption. This mobility effect is specific to each class of dye [50]. Furthermore, [58, 59] explained that with increasing temperature, the thickness of the boundary layer surrounding the adsorbent is reduced. Thus, the resistance to mass transfer of the adsorbate in the boundary layer decreases, which promotes adsorption.
In order to confirm whether the adsorption process of carmoisine on ND is endothermic, the thermodynamic parameters, Gibbs free energy $\Delta G°$, enthalpy $\Delta H°$, and change in entropy $\Delta S°$ were determined from Equations (6)–(8).

$$\Delta G° = -RT.\ln Kd. \qquad (6)$$

Here, R is the universal gas constant ($8.314 \, J \, mol^{-1}°K$), and T is the absolute temperature (K). The apparent
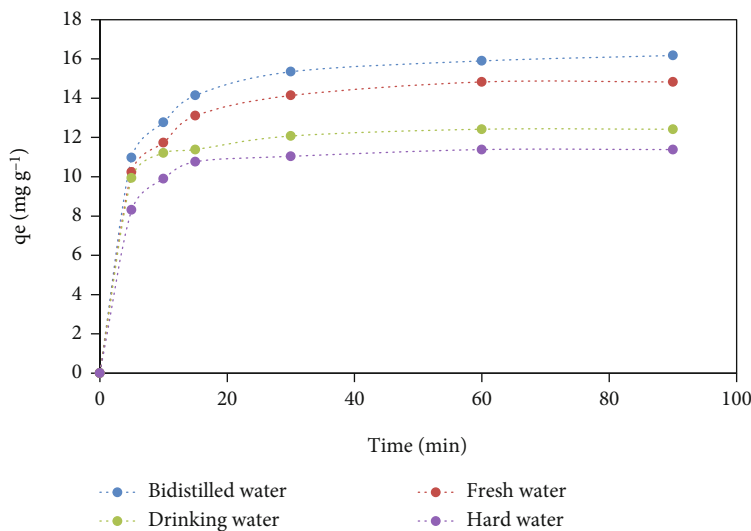
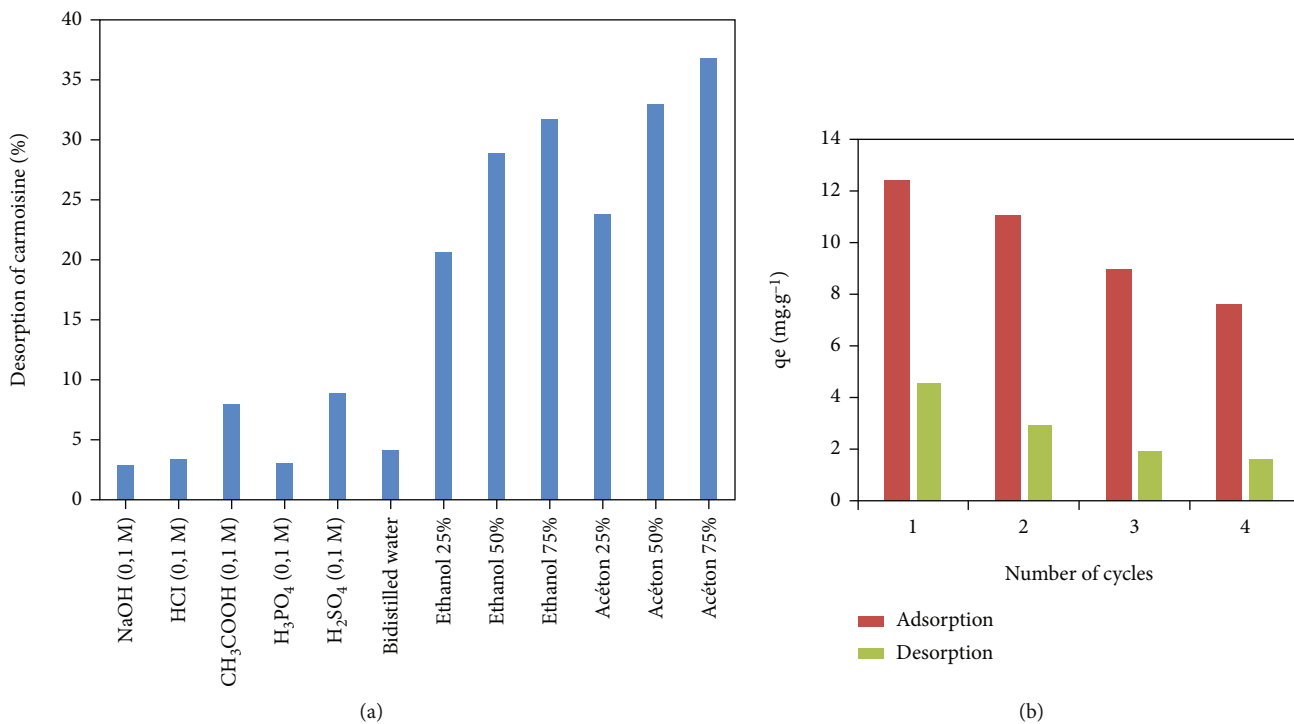FIGURE 10: Effect of hardness and mineralization of water on the adsorption efficiency of carmoisine on ND.

FIGURE 11: Desorption of carmoisine using (a) different eluents and (b) acetone (50%) after 4 cycles.

equilibrium constant Kd ($L g^{-1}$) of the adsorption is defined as follows.

$$Kd = \frac{qe}{ce}, \qquad (7)$$

where q_e and C_e are the equilibrium concentrations of carmoisine for the LND ($mg g^{-1}$) and the solution ($mg L^{-1}$), respectively.

$$\ln Kd = -\frac{\Delta Go}{RT} = \frac{\Delta So}{R} - \frac{\Delta Ho}{R} \cdot \left(\frac{1}{T}\right). \qquad (8)$$

The $\Delta H°$ and $\Delta S°$ values can be obtained from the slope and intercept of the Van't Hoff plots of lnKd versus 1/T Figure 9. The shape of the curve is considered satisfactory due to the correlation coefficient obtained.

The values of $\Delta G°$, $\Delta H°$, and $\Delta S°$ are given in Table 2. Whatever the temperature tested, $\Delta G°$ is negative, indicating the spontaneous nature of carmoisine adsorption on ND. The positive value of $\Delta H°$ indicates the endothermic nature of the adsorption with a strong interaction of carmoisine with ND. In addition, the positive value of $\Delta S°$ suggests that the randomness at the adsorbent/adsorbate interface increases during the adsorption of carmoisine by ND.

TABLE 4: Comparison of adsorption capacities of various adsorbents for removal of carmoisine (Cne).

Biosorbents	Removal conditions						
	Initial pH	Adsorbent dose (gL^{-1})	C0 (Cne) (mgL^{-1})	T (°C)	tc (min)	qe (mgg^{-1})	References
Polypyrrole coated onto sawdust (PPy/SD)	4	1	100	25	60	2.48	[65]
Bottom ash	2.5	4	50	50	333	8.63	[3]
Modified activated carbon	4.8	4.8	50	20	60	2.5	[66]
Feldspar	2	2	150	20	90	3.98	[67]
ND	1	1	50	20	60	12	This study

TABLE 5: Parameters of adsorption models applied in adsorption of the carmoisine on ND.

| Isotherm model	Equation (number)	Parameters	10 °C	20 °C	30 °C	40 °C	50 °C
Langmuir	Nonlinear form $q_e = q_{\max K_L C_e}/1 + K_L C_e (10)$ Linear form $1/q_e = (1/q_{\max}) + \left(1/q_{\max K_L C_e}\right)(11)$ Plot $1/C_e$ vs $1/q_e$	$q_{\max}$ (mgg^{-1})	7.75	24.21	21.36	16.58	16.77
		K_L (Lmg^{-1})	0.0138	0.0090	0.0117	0.0142	0.0153
		R^2	0.993	0.999	0.999	0.999	0.998
		χ^2	111.6	23.03	36.77	57.2	58.97
Freundlich	Nonlinear form $q_e = K_F C_e^{1/n_F}(12)$ Linear form $\log q_e = \log K_F + (1/n_F) \log C_e(13)$ Plot $\log C_e$ vs $\log q_e$	K_F ($mg^{1-1/n}L^{1/n}g^{-1}$)	0.044	0.169	0.170	0.171	0.2
		R^2	0.932	0.996	0.986	0.993	0.993
		n ($mgg min^{-1}$)	0.671	0.926	0.813	0.798	0.812
		χ^2	3.846	0.0981	1.936	0.499	0.565

Nomenclature: q_e and $q_{\max}$ are the amount of dye adsorbed per unit at equilibrium and the maximum amount of adsorption, respectively (mgg^{-1}). C_e is the concentration of dye solution at equilibrium (mgL^{-1}). K_F, n_F, and K_L are constants of adsorption isotherms.

3.2.5. Hardness Effect and Mineralization of Water.
To take into account the effects of hardness and mineralization or conductivity of water on the adsorption of carmoisine on ND, the samples of dye prepared in double-distilled water and water of increasing hardness have been tested Table 3. The results given in Figure 10 show that increasing the hardness and mineralization of the water adversely affects the color removal efficiency on ND. More precisely, for a contact time of 60 min, the adsorption capacity of carmoisine goes from ~16 mgg^{-1} for bidistilled water to ~11 mgg^{-1} for very hard water. The reduction in efficiency observed could be attributed in particular to the competition between and CO_3^{2-} of water and SO_3^- of carmoisine for the same reactive sites on the surface of LND. On the other hand, a passivation effect on the surface of ND would be possible by forming complexes and surface precipitates with aluminum and silica, which are the main constituents of ND. This surface passivation of the material was reported by [60] but for nZVI/ Pd bimetallic nanoparticles supported by clay, used to remove methyl orange from an aqueous solution.

3.2.6. Study of the ND Regeneration and Wear.
This study aims to evaluate the rate of adsorption and desorption of the dye or the rate of regeneration of the biomaterial and also to note the number of cycles of adsorption/desorption or wear of this biomaterial. All the experiments were carried out after saturation of the ND at 1 gL^{-1} with an initial solution of carmoisine at 50 mgL^{-1}, pH 2 ± 0.1, and 21 ± 0.5 °C. The results in Figure 11(a) show that in an acid medium, the desorption is sensibly greater than that in a basic medium. This behavior was predictable given the protonation of the surface of the ND in an acid medium and the anionic nature of the carmoisine marked by the sulfonates. Furthermore, the use of organic solvents quantitatively increases the desorption of the carmoisine of the adsorbent, especially for acetone where the desorption rate is about 35%. A repulsive deprotonation would be at the origin of this desorption of the carmoisine of the material. A deprotonation is carried out both on the carmoisine molecule where all the bonds are involved (-N=N-, -OH, and -SO_3) and on the surface of the ND. Ethanol would become the ethalonate ion ($C_2H_5O^-$) and acetone and the enolate ion ($C_3H_5O^-$) causing considerable desorption compared to the use of mineral eluents or bidistilled water. For the study of the number of cycles of adsorption/desorption or regeneration, acetone at 50% was tested as being the best eluent. This eluent was also used by [11] during the regeneration and wear of date stones by Rouge Congo. The results given in Figure 11(b) show that regeneration is possible but not satisfactory. ND wear is observed from one cycle to the next. Indeed, the adsorption capacity of carmoisine on ND is reduced by around 50% after the 4th cycle. This loss of performance of all adsorbent materials is recognized by many authors [61, 62].

The wear of the material is frequently explained by the loss of active sites on the surface of the adsorbent [61, 63]. This loss of effectiveness of the material over time does not discourage its use given its abundance. The comparison of
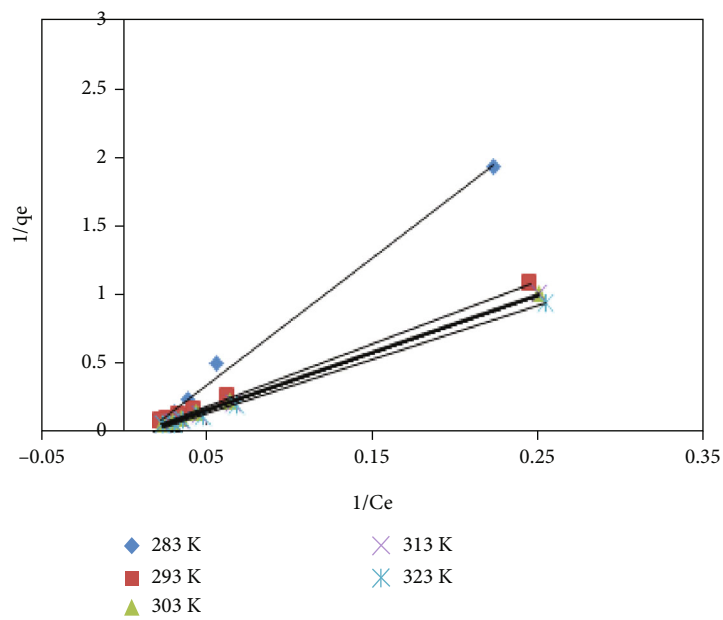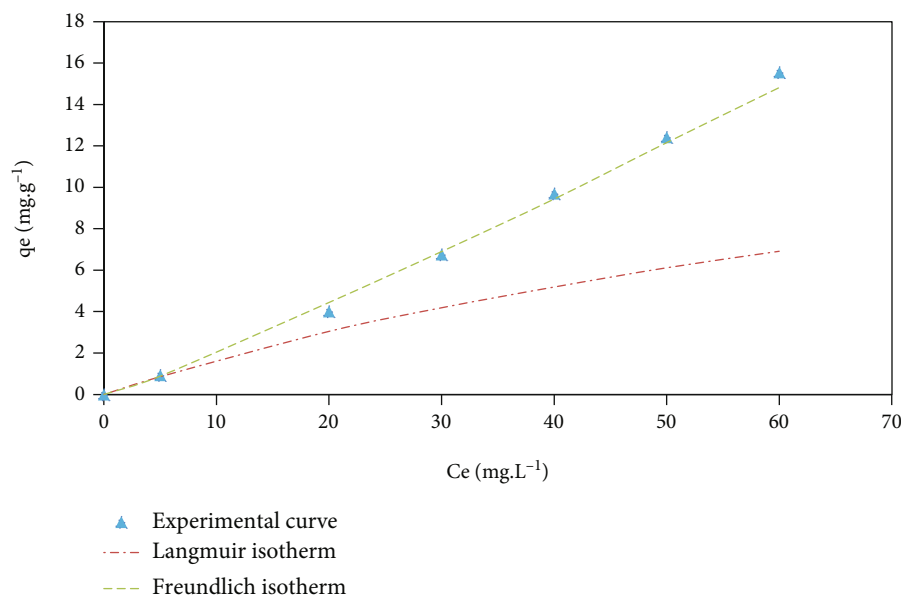
(a)
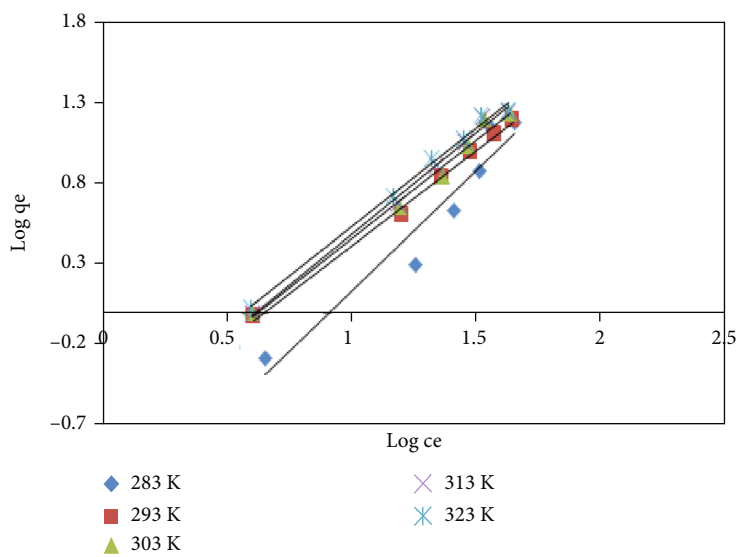
(b)

FIGURE 12: Continued.

(c)

FIGURE 12: Plots of (a) Langmuir, (b) Freundlich, and (c) experimental data (at 20 °C) for the adsorption of carmoisine onto ND.

TABLE 6: Parameters of kinetic models applied in adsorption of the carmoisine at 20°C.

(a)

Kinetic model	Equation number	Parameters				
		$[Cne]$ (mg L^{-1})	q_{ee} (mg g^{-1})	q_{ec} (mg g-1)	k_1 (min^{-1})	R^2
Pseudo-first order	Non-linear form $dq_t/dt = k_1(q_e - q_t)(14)$ Linear form $\log(q_e - q_t) = \log q_e - k_1.t/2.303(15)$ Plot $\log(q_e - q_t)$ vs t	5	0.93	0.20	0.008	0.071
		20	4	0.22	0.043	0.778
		30	6.75	2.55	0.022	0.810
		40	9.68	2.87	0.018	0.687
		50	12.41	2.73	0.011	0.686
		60	15.55	2.58	0.013	0.584

(b)

|		$[Cne]$ (mg L^{-1})	q_{ee} (mg g^{-1})	q_{ec} (mg g^{-1})	k_2 (min^{-1})	R^2	h (mg g^{-1} min)
Pseudo-second order	Non-linear form $dq_t/dt = k_2(q_e - q_t)2(16)$ Linear form $t/q_t = (1/k_2q_e^2) + (t/q_e)(17)$ Plot $\frac{t}{q_t}$ vs t $h = k_2q_e^2(18)$	5	0.93	0.97	0.92	0.900	0.169
		20	4	4.21	0.084	0.999	1.504
		30	6.75	7.25	0.029	0.997	1.524
		40	9.68	10.27	0.029	0.996	3.058
		50	12.41	12.69	0.0719	0.999	11.57
		60	15.55	16.55	0.0172	0.998	4.711

Nomenclature: q_e and q_t are amount of dye adsorbed per unit of adsorbent at equilibrium and at time t, respectively(mg g^{-1}). k_1 and k_2 are the pseudo-first-order and pseudo-second-order rate constants, respectively. h: initial adsorption rate.

the adsorption capacity of carmoisine on ND with other natural and composite biomaterials shows Table 4 that is competitive and can therefore be potentially used as a low-cost biosorbent for the elimination of carmoisine from an aqueous solution. However, direct comparison of adsorption

capacities is not always easy due to the different experimental conditions used in each study. On the other hand, these treatments generate in all cases a sludge containing the adsorbent and residues of the dye and other chemical additives. This constitutes a major drawback of the use of this
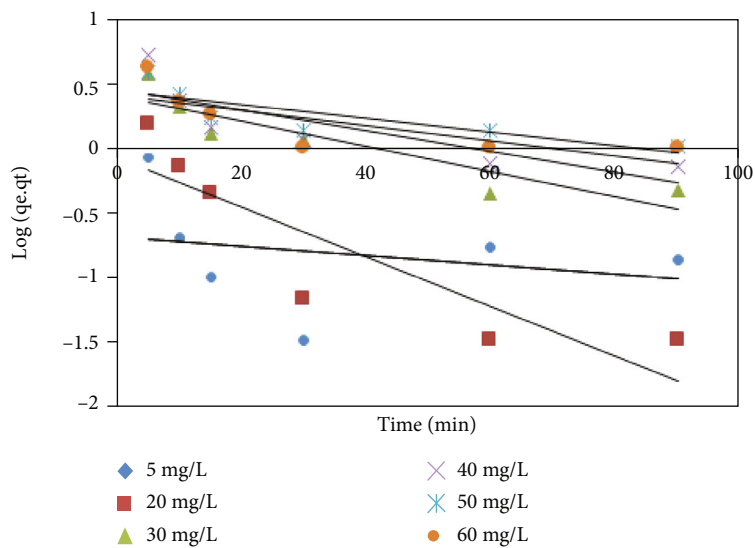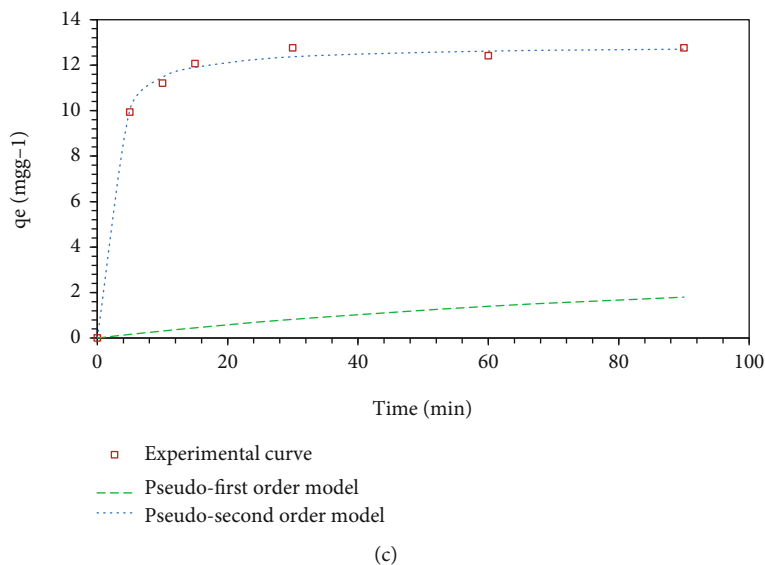
(a)
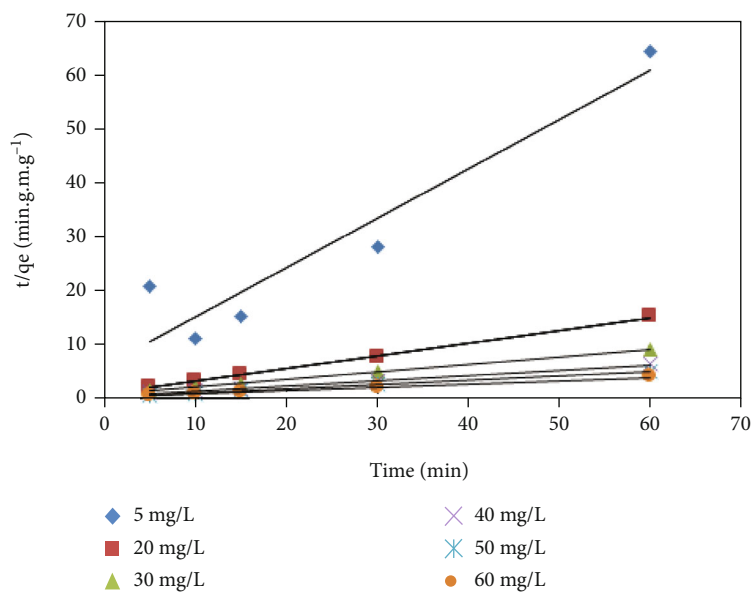
(b)

FIGURE 13: Continued.

(c)

FIGURE 13: Plots of (a) pseudo-first-order kinetic, (b) pseudo-second-order kinetic, (c) and experimental data.

adsorption technique. However, coupling with electrochemical techniques is an innovative alternative to solve this problem [61, 64].

3.3. Modeling of Adsorption.

The advantage of adsorption isotherms is that they show the distribution of adsorbent molecules on the surface of the adsorbent under equilibrium conditions and the effect of concentration at equilibrium on the loading capacity at different temperatures [68].

Thus, the modeling of experimental data by the use of linear and nonlinear regression models like those of Langmuir, Freundlich, Brunauer-Emmett-Teller, Redlich-Peterson, Dubinin-Radushkevich, Temkin, Toth, Koble-Corrigan, Sips, Flory-Huggins, and Radke-Prausnitz makes it possible to provide valuable information such as the nature of the adsorption (monolayer and multilayer), the adsorbent/adsorbate interaction mechanisms, the surface properties, and the degree of affinity of the adsorbent [69].

The models tested in this study are those frequently used in adsorption, namely the Langmuir and Freundlich models represented by their respective equations in Table 5.

The adsorption modeling was carried out on the basis of the experimental results in Figure 8, at variable temperatures (283 to 323°K), with an initial concentration of carmoisine at $50 \, \text{mgL}^{-1}$ and at free pH. The results of the modeling and the adsorption parameters are shown in Figures 12(a)–12(c) and Table 5. They clearly show that Freundlich model most closely reflects the experimental results. Indeed, a good linearization of the curves is observed with correlation coefficients close to the unit and very low chi^2 tests (3.846 to 0.565). The results given in Figure 12(c), conducted at an ambient temperature at 293°K, a concentration of $50 \, \text{mg L}^{-1}$ in carmoisine, pH = 2, and a ND concentration of $1 \, \text{g L}^{-1}$, confirm the application of the model of Freundlich to represent the experimental results. The Freundlich constant (K_F) increases with temperature increasing, which indicates that the adsorption of carmoisine on ND is favorable. This increase in K_F with temperature confirms the endothermic

nature of the adsorption process. Thus, the adsorption process would occur on a heterogeneous surface or on heterogeneous adsorption sites [70].

3.4. Kinetic Modeling.

Adsorption kinetics are important to follow, as they provide valuable information on the effectiveness of the treatment and the design of adsorption systems.

They are of considerable practical interest for the implementation of an industrial adsorbent. It is expressed in terms of the rate of solute retention as a function of the contact time. The speed with which thermodynamic equilibrium is reached is a function of the adsorbate diffusion rate and the adsorbate-adsorbent interaction [71, 72].

To this end, the experimental data in Figure 7 are analyzed using the kinetic models of pseudo-first order and pseudo-second order equations indicated in Table 6. These two models are widely studied and compared; the first explains the adsorption of the adsorbate on the adsorbent according to the first-order mechanism indicated by the corresponding equation, while the second assumes that the rate of adsorption of the adsorbate is proportional to the sites available on the adsorbent [73].

The results of the modeling and kinetic parameters are summarized in Figures 13(a)–13(c) and Table 6. They clearly show that the pseudo-second-order model best represents the experimental results. Indeed, for each of the concentrations of carmoisine tested (5 to $60 \, \text{mg L}^{-1}$), the experimental adsorption capacity (q_{ee}) is close to that calculated (q_{ec}). Good linearization of the curves is observed with correlation coefficients close to unity. It is also noted that with the increase in the carmoisine concentration in Table 6, h and q_e increase, and then K_2 decreases. This behavior would be linked to the increase in the driving force for mass transfer. The results in Figure 13(c), obtained from the carmoisine concentration test of $50 \, \text{mg L}^{-1}$, a temperature of 293°K, and an ND concentration of $1 \, \text{g L}^{-1}$, confirm the right fit to pseudo-second-order kinetics. Similar results and trends

have been reported by different authors on natural and pre-treated diatomites but on other dyes [74, 75].

4. Conclusion

This work focuses, for the first time, on the use of a natural diatomite (ND) in removing the azo dye carmoisine, high-risk food coloring agent for consumer health, by adsorption process. The physicochemical characterization show that ND is mainly composed of silica with a fraction of calcite and ankerite minerals. The ND adsorbent is porous with a specific surface of about $41 \, m^2 g$ with a hydroxyl surface functional group -OH.

Adsorption process on ND was found to be effective in removing the carmoisine colorant. The adsorption capacity is strongly influenced by the adsorbent and adsorbate contents, the solution pH, the work temperature, and the water hardness and mineralization. The maximum of adsorption capacity, as function of temperature, was between 15 and $12 \, mg \, g^{-1}$. At room temperature, optimal experimental conditions for the highest adsorption capacity ($12 \, mg.g^{-1}$) was colorant concentration $50 \, mg.L^{-1}$, pH 2, contact time 30 min, and ND content $1 \, g.L^{-1}$.

Modeling study has shown that experimental results are well modeled by the Freundlich isotherm in multilayer adsorption. The reaction kinetics are pseudo-second order, and the thermodynamic parameters indicated that the nature of the adsorption process is endothermic and spontaneous. This study suggests that adsorption treatment using abundant and inexpensive ND could be considered as a practical, rapid, and economical alternative for the removal of carmoisine and more widely anionic azo dyes.

Data Availability

There is no data supporting this study.

Conflicts of Interest

The authors declare no conflicts of interest.

Acknowledgments

References

[1] E. H. Koupaie, M. A. Moghaddam, and S. Hashemi, "Post-treatment of anaerobically degraded azo dye Acid Red 18 using aerobic moving bed biofilm process: enhanced removal of aromatic amines," *Journal of Hazardous Materials*, vol. 195, pp. 147–154, 2011.

[2] B. G. Li, S. Y. Han, and R. Teng, "Adsorption of acid carmoisine B by fly ash/chitosan composite," *Materials Science Forum*, vol. 847, pp. 224–229, 2016.

[3] V. K. Gupta, A. Mittal, A. Malviya, and J. Mittal, "Adsorption of carmoisine A from wastewater using waste materials–bottom ash and deoiled soya," *Journal of Colloid and Interface Science*, vol. 335, no. 1, pp. 24–33, 2009.

[4] F. Jy and N. Elgendy, "Performance, kinetics and equilibrium in biosorption of anionic dye Acid Red 14 by the waste biomass of Saccharomyces cerevisiae as a low-cost biosorbent," *Turkish Journal of Engineering and Environmental Sciences*, vol. 37, pp. 146–161, 2013.

[5] H. Roth, Y. Gendel, P. Buzatu, O. David, and M. Wessling, "Tubular carbon nanotube-based gas diffusion electrode removes persistent organic pollutants by a cyclic adsorption-electro-Fenton process," *Journal of Hazardous Materials*, vol. 307, pp. 1–6, 2016.

[6] M. A. Salem, S. T. Abdel-Halim, A. E.-H. M. El-Sawy, and A. B. Zaki, "Kinetics of degradation of allura red, ponceau 4R and carmosine dyes with potassium ferrioxalate complex in the presence of H_2O_2," *Chemosphere*, vol. 76, no. 8, pp. 1088–1093, 2009.

[7] H. Gao, S. Zhao, X. Cheng, X. Wang, and L. Zheng, "Removal of anionic azo dyes from aqueous solution using magnetic polymer multi-wall carbon nanotube nanocomposite as adsorbent," *Chemical Engineering Journal*, vol. 223, pp. 84–90, 2013.

[8] L. Zheng, C. Wang, Y. Shu, X. Yan, and L. Li, "Utilization of diatomite/chitosan-Fe (III) composite for the removal of anionic azo dyes from wastewater: equilibrium, kinetics and thermodynamics," *Colloids and Surfaces A: Physicochemical and Engineering Aspects*, vol. 468, pp. 129–139, 2015.

[9] A. Baddouh, G. G. Bessegato, M. M. Rguiti et al., "Electrochemical decolorization of Rhodamine B dye: influence of anode material, chloride concentration and current density," *Journal of Environmental Chemical Engineering*, vol. 6, no. 2, pp. 2041–2047, 2018.

[10] F. Z. Khelaifia, S. Hazourli, S. Nouacer, H. Rahima, and M. Ziati, "Valorization of raw biomaterial waste-date stones for Cr (VI) adsorption in aqueous solution: thermodynamics, kinetics and regeneration studies," *International Biodeterioration & Biodegradation*, vol. 114, pp. 76–86, 2016.

[11] R. Hachani, H. Sabir, N. Sana, K. F. Zohra, and N. M. Nesrine, "Performance study of a low-cost adsorbent—raw date pits—-for removal of azo dye in aqueous solution," *Water Environment Research*, vol. 89, no. 9, pp. 827–839, 2017.

[12] K. R. Kalash and T. M. Albayati, "Remediation of oil refinery wastewater implementing functionalized mesoporous materials MCM-41 in batch and continuous adsorption process," *Desalination and Water Treatment*, vol. 220, pp. 130–141, 2021.

[13] A. R. Kul, A. Aldemir, and H. Koyuncu, "An investigation of natural and modified diatomite performance for adsorption of Basic Blue 41: isotherm, kinetic, and thermodynamic studies," *Desalination and Water Treatment*, vol. 229, pp. 384–394, 2021.

[14] W. Yang, P. J. Lopez, and G. Rosengarten, "Diatoms: self assembled silica nanostructures, and templates for bio/chemical sensors and biomimetic membranes," *Analyst*, vol. 136, no. 1, pp. 42–53, 2011.

[15] S. Kabiri, M. D. Kurkuri, T. Kumeria, and D. Losic, "Frit-free PDMS microfluidic device for chromatographic separation

and on-chip detection," *RSC Advances*, vol. 4, no. 29, pp. 15276–15280, 2014.

[16] X. W. Sun, Y. X. Zhang, and D. Losic, "Diatom silica, an emerging biomaterial for energy conversion and storage," *Journal of Materials Chemistry A*, vol. 5, no. 19, pp. 8847–8859, 2017.

[17] G. Sriram, M. Kigga, U. Uthappa et al., "Naturally available diatomite and their surface modification for the removal of hazardous dye and metal ions: a review," *Advances in Colloid and Interface Science*, vol. 282, article 102198, 2020.

[18] J. Lin, S. Zhan, M. Fang, and X. Qian, "The adsorption of dyes from aqueous solution using diatomite," *Journal of Porous Materials*, vol. 14, no. 4, pp. 449–455, 2007.

[19] D. Nikjoo, V. Perrot, and F. Akhtar, "Laminated porous diatomite monoliths for adsorption of dyes from water," *Environmental Progress & Sustainable Energy*, vol. 38, no. s1, pp. S377–S385, 2019.

[20] A. Touina, S. Chernai, B. Mansour, H. Hadjar, A. Ouakouak, and B. Hamdi, "Characterization and efficient dye discoloration of Algerian diatomite from Ouled Djilali-Mostaganem," *SN Applied Sciences*, vol. 3, no. 4, pp. 1–13, 2021.

[21] A. Rai, V. Sirotiya, M. Mourya et al., "Sustainable treatment of dye wastewater by recycling microalgal and diatom biogenic materials: biorefinery perspectives," *Chemosphere*, vol. 305, p. 135371, 2022.

[22] F. Aguilar, U. R. Charrondiere, B. Dusemund et al., "Scientific opinion on the re-evaluation of azorubine/carmoisine (E 122) as a food additive," *EFSA Journal*, vol. 7, no. 11, 2009.

[23] Joint F, Additives WECoF, and Organization WH, *Safety evaluation of certain food additives and contaminants: prepared by the seventy fourth meeting of the Joint FAO/WHO Expert Committee on Food Additives (JECFA)*, World Health Organization, 2012.

[24] M. Diezi, T. Buclin, and J. Diezi, "Additifs alimentaires et troubles de l'attention/hyperactivité chez l'enfant," *Paediatrica*, vol. 22, pp. 12–15, 2011.

[25] J. M. Obón, J. M. Angosto, F. González-Soto, A. Ascua, and J. A. Fernández-López, "Prototyping a spinning adsorber submerged filter for continuous removal of wastewater contaminants," *Journal of Water Process Engineering*, vol. 45, article 102515, 2022.

[26] M. Shams, H. Balouchi, H. Alidadi et al., "Coupling electrocoagulation and solar photocatalysis for electro- and photo- catalytic removal of carmoisine by Ag/graphitic carbon nitride: Optimization by process modeling and kinetic studies," *Journal of Molecular Liquids*, vol. 340, article 116917, 2021.

[27] Z. Kiayi, T. B. Lotfabad, A. Heidarinasab, and F. Shahcheraghi, "Microbial degradation of azo dye carmoisine in aqueous medium using Saccharomyces cerevisiae ATCC 9763," *Journal of Hazardous Materials*, vol. 373, pp. 608–619, 2019.

[28] H. Barrera, J. Cruz-Olivares, B. A. Frontana-Uribe, A. Gómez-Díaz, P. G. Reyes-Romero, and C. E. Barrera-Diaz, "Electro-oxidation–plasma treatment for azo dye carmoisine (Acid Red 14) in an aqueous solution," *Materials*, vol. 13, no. 6, p. 1463, 2020.

[29] A. Wakrim, A. Dassaa, Z. Zaroual, S. E. Ghachtouli, J. J. Eddine, and M. Azzi, "Mechanistic study of carmoisine dye degradation in aqueous solution by Fenton process," *Materials Today: Proceedings*, vol. 37, pp. 3847–3853, 2021.

[30] M. Bendaia, S. Hazourli, A. Aitbara, and M. N. Nait, "Performance of electrocoagulation for food azo dyes treatment in

aqueous solution: optimization, kinetics, isotherms, thermodynamic study and mechanisms," *Separation Science and Technology*, vol. 56, no. 12, pp. 2087–2103, 2021.

[31] S. Brauneur, P. Emmet, and E. Teller, "Adsorption of gases in multimolecular layers," *Journal of the American Chemical Society*, vol. 60, no. 2, pp. 309–319, 1938.

[32] H. J. Al-Jaaf, N. S. Ali, S. M. Alardhi, and T. M. Albayati, "Implementing of eggplant peels as an efficient bio-adsorbent for treatment of oily domestic wastewater," *Desalination and Water Treatment*, vol. 245, pp. 226–237, 2022.

[33] Y. A. Abd Al-Khodor and T. M. Albayati, "Employing sodium hydroxide in desulfurization of the actual heavy crude oil: theoretical optimization and experimental evaluation," *Process Safety and Environmental Protection*, vol. 136, pp. 334–342, 2020.

[34] S. Lagergren, "Zur theorie der sogenannten adsorption geloster stoffe," *Handlingar*, vol. 24, pp. 1–39, 1898.

[35] Y.-S. Ho and G. McKay, "Pseudo-second order model for sorption processes," *Process Biochemistry*, vol. 34, no. 5, pp. 451–465, 1999.

[36] I. Langmuir, "The adsorption of gases on plane surfaces of glass, mica and platinum," *Journal of the American Chemical Society*, vol. 40, no. 9, pp. 1361–1403, 1918.

[37] H. Freundlich, "Over the adsorption in solution," *The Journal of Physical Chemistry*, vol. 57, pp. 1100–1107, 1906.

[38] Y. Zhou, J. Lu, Y. Zhou, and Y. Liu, "Recent advances for dyes removal using novel adsorbents: a review," *Environmental Pollution*, vol. 252, no. Partt A, pp. 352–365, 2019.

[39] H. F. Alazzawi, I. K. Salih, and T. M. Albayati, "Drug delivery of amoxicillin molecule as a suggested treatment for COVID-19 implementing functionalized mesoporous SBA-15 with aminopropyl groups," *Drug Delivery*, vol. 28, no. 1, pp. 856–864, 2021.

[40] S. S. Ibrahim and A. Q. Selim, "Evaluation of Egyptian diatomite for filter aid applications," *Physicochemical Problems of Mineral Processing*, vol. 47, pp. 113–122, 2011.

[41] K. Khaldi, M. Hadjel, R. Cherrak, Z. Souidi, and A. Benyoucef, "Adsorption kinetics of an cationic dye ffrom aqueouse solution by Algerian mineral materials," *Moroccan Journal of Chemistry*, vol. 6, no. 6-2, pp. 2227–2236, 2018.

[42] M. Aivalioti, P. Papoulias, A. Kousaiti, and E. Gidarakos, "Adsorption of BTEX, MTBE and TAME on natural and modified diatomite," *Journal of Hazardous Materials*, vol. 207-208, pp. 117–127, 2012.

[43] Y. Du, X. Wang, J. Wu, J. Wang, Y. Li, and H. Dai, "$Mg_3Si_4O_{10}(OH)_2$ and $MgFe_2O_4$ in situ grown on diatomite: Highly efficient adsorbents for the removal of Cr(VI)," *Microporous and Mesoporous Materials*, vol. 271, pp. 83–91, 2018.

[44] B. Zhu, K. Qiu, C. Shang, and Z. Guo, "Naturally derived porous carbon with selective metal- and/or nitrogen-doping for efficient CO2 capture and oxygen reduction," *Journal of Materials Chemistry A*, vol. 3, no. 9, pp. 5212–5222, 2015.

[45] P. Vasconcelos, J. Labrincha, and J. Ferreira, "Permeability of diatomite layers processed by different colloidal techniques," *Journal of the European Ceramic Society*, vol. 20, no. 2, pp. 201–207, 2000.

[46] A. Sarı, D. Çıtak, and M. Tuzen, "Equilibrium, thermodynamic and kinetic studies on adsorption of Sb(III) from aqueous solution using low-cost natural diatomite," *Chemical Engineering Journal*, vol. 162, no. 2, pp. 521–527, 2010.

[47] N. Inchaurrondo, J. Font, C. P. Ramos, and P. Haure, "Natural diatomites: efficient green catalyst for Fenton-like oxidation of

Orange II," *Applied Catalysis B: Environmental*, vol. 181, pp. 481–494, 2016.

[48] M. T. Yagub, T. K. Sen, S. Afroze, and H. M. Ang, "Dye and its removal from aqueous solution by adsorption: a review," *Advances in Colloid and Interface Science*, vol. 209, pp. 172–184, 2014.

[49] M. Foroughi-Dahr, H. Abolghasemi, M. Esmaili, A. Shojamoradi, and H. Fatoorehchi, "Adsorption characteristics of Congo red from aqueous solution onto tea waste," *Chemical Engineering Communications*, vol. 202, no. 2, pp. 181–193, 2015.

[50] M. A. M. Salleh, D. K. Mahmoud, W. A. W. A. Karim, and A. Idris, "Cationic and anionic dye adsorption by agricultural solid wastes: a comprehensive review," *Desalination*, vol. 280, no. 1-3, pp. 1–13, 2011.

[51] V. S. Munagapati, V. Yarramuthi, Y. Kim, K. M. Lee, and D.-S. Kim, "Removal of anionic dyes (Reactive Black 5 and Congo Red) from aqueous solutions using banana peel powder as an adsorbent," *Ecotoxicology and Environmental Safety*, vol. 148, pp. 601–607, 2018.

[52] H. A. Alyosef, S. Ibrahim, J. Welscher et al., "Effect of acid treatment on the chemical composition and the structure of Egyptian diatomite," *International Journal of Mineral Processing*, vol. 132, pp. 17–25, 2014.

[53] V. S. Mane, I. D. Mall, and V. C. Srivastava, "Kinetic and equilibrium isotherm studies for the adsorptive removal of brilliant green dye from aqueous solution by rice husk ash," *Journal of Environmental Management*, vol. 84, no. 4, pp. 390–400, 2007.

[54] Q. Baocheng, Z. Jiti, X. Xiang, C. Zheng, Z. Hongxia, and Z. Xiaobai, "Adsorption behavior of azo dye C. I. acid red 14 in aqueous solution on surface soils," *Journal of Environmental Sciences*, vol. 20, no. 6, pp. 704–709, 2008.

[55] S. Nouacer, S. Hazourli, R. Djellabi, F. Khlaifia, R. Hachani, and M. Ziati, "Using a new lignocellulosic material based on palm stems for hexavalent chromium adsorption in aqueous solution," *International Journal of Environmental Research*, vol. 10, pp. 41–50, 2016.

[56] M. Ziati and S. Hazourli, "Removal of chemical oxygen demand from pharmaceutical wastewater by adsorption on anthracite. Adsorption isotherms and thermodynamics," *Revue Roumaine de Chimie*, vol. 62, pp. 933–940, 2017.

[57] E. H. Khader, T. J. Mohammed, and T. M. Albayati, "Comparative performance between rice husk and granular activated carbon for the removal of azo tartrazine dye from aqueous solution," *Desalination and Water Treatment*, vol. 229, pp. 372–383, 2021.

[58] S. Aytas, M. Yurtlu, and R. Donat, "Adsorption characteristic of U(VI) ion onto thermally activated bentonite," *Journal of Hazardous Materials*, vol. 172, no. 2-3, pp. 667–674, 2009.

[59] B. Singha and S. K. Das, "Biosorption of Cr(VI) ions from aqueous solutions: kinetics, equilibrium, thermodynamics and desorption studies," *Colloids and Surfaces B: Biointerfaces*, vol. 84, no. 1, pp. 221–232, 2011.

[60] T. Wang, J. Su, X. Jin, Z. Chen, M. Megharaj, and R. Naidu, "Functional clay supported bimetallic nZVI/Pd nanoparticles used for removal of methyl orange from aqueous solution," *Journal of Hazardous Materials*, vol. 262, pp. 819–825, 2013.

[61] S. Hazourli, G. Bonnecaze, and M. Astruc, "Adsorption et electrosorption de composes organiques Sur charbon actif en grains partie I-influence du Potentiel impose et du nombre de cycles adsorption and electrosorption of organic compounds on granular activated carbon part I-influence of applied potential and number of cycles," *Environmental Technology*, vol. 17, no. 12, pp. 1275–1283, 1996.

[62] V. Gupta and A. Rastogi, "Biosorption of hexavalent chromium by raw and acid-treated green alga Oedogonium hatei from aqueous solutions," *Journal of Hazardous Materials*, vol. 163, no. 1, pp. 396–402, 2009.

[63] S. Hazourli, G. Bonnecaze, and M. Astruc, "Influence de divers traitements sur les groupements oxygenes superficiels et le potentiel d'un charbon actif en grains," *Carbon*, vol. 32, no. 3, pp. 523–535, 1994.

[64] M. Cherifi, S. Hazourli, S. Pontvianne, F. Lapicque, and J.-P. Leclerc, "Electrokinetic removal of aluminum and chromium from industrial wastewater electrocoagulation treatment sludge," *Desalination and Water Treatment*, vol. 57, no. 39, pp. 18500–18515, 2016.

[65] R. Ansari, M. B. Keivani, and A. F. Delavar, "Application of polypyrrole coated onto wood sawdust for the removal of carmoisine dye from aqueous solutions," *Journal of Applied Polymer Science*, vol. 122, no. 2, pp. 804–812, 2011.

[66] M. Yazdani, N. M. Mahmoodi, M. Arami, and H. Bahrami, "Surfactant-modified feldspar: isotherm, kinetic, and thermodynamic of binary system dye removal," *Journal of Applied Polymer Science*, vol. 126, no. 1, pp. 340–349, 2012.

[67] S. Yan, W. Huo, J. Yang et al., "Green synthesis and influence of calcined temperature on the formation of novel porous diatomite microspheres for efficient adsorption of dyes," *Powder Technology*, vol. 329, pp. 260–269, 2018.

[68] B. Hameed, I. Tan, and A. Ahmad, "Adsorption isotherm, kinetic modeling and mechanism of 2,4,6-trichlorophenol on coconut husk-based activated carbon," *Chemical Engineering Journal*, vol. 144, no. 2, pp. 235–244, 2008.

[69] N. Ayawei, A. N. Ebelegi, and D. Wankasi, "Modelling and interpretation of adsorption isotherms," *Journal of Chemistry*, vol. 2017, Article ID 3039817, 11 pages, 2017.

[70] V. Vimonses, S. Lei, B. Jin, C. W. Chow, and C. Saint, "Kinetic study and equilibrium isotherm analysis of Congo red adsorption by clay materials," *Chemical Engineering Journal*, vol. 148, no. 2-3, pp. 354–364, 2009.

[71] J.-P. Simonin, "On the comparison of pseudo-first order and pseudo-second order rate laws in the modeling of adsorption kinetics," *Chemical Engineering Journal*, vol. 300, pp. 254–263, 2016.

[72] A. T. Khadim, T. M. Albayati, and N. M. C. Saady, "Desulfurization of actual diesel fuel onto modified mesoporous material Co/MCM-41," *Environmental Nanotechnology, Monitoring & Management*, vol. 17, article 100635, 2022.

[73] S. T. Kadhum, G. Y. Alkindi, and T. M. Albayati, "Eco friendly adsorbents for removal of phenol from aqueous solution employing nanoparticle zero-valent iron synthesized from modified green tea bio-waste and supported on silty clay," *Chinese Journal of Chemical Engineering*, vol. 36, pp. 19–28, 2021.

[74] B. Hayati and N. M. Mahmoodi, "Modification of activated carbon by the alkaline treatment to remove the dyes from wastewater: mechanism, isotherm and kinetic," *Desalination and Water Treatment*, vol. 47, no. 1-3, pp. 322–333, 2012.

[75] M. A. Al-Ghouti, M. A. Khraisheh, M. N. Ahmad, and S. Allen, "Adsorption behaviour of methylene blue onto Jordanian diatomite: a kinetic study," *Journal of Hazardous Materials*, vol. 165, no. 1-3, pp. 589–598, 2009.